Neuron 52, 623–634, November 22, 2006 ©2006 Elsevier Inc. DOI 10.1016/j.neuron.2006.10.005

Functional Interactions at the Interface between Voltage-Sensing and Pore Domains in the Shaker K_v Channel

Gilberto J. Soler-Llavina,[1,2] Tsg-Hui Chang,[1] and Kenton J. Swartz[1,*]
[1] Molecular Physiology and Biophysics Section
Porter Neuroscience Research Center
National Institute of Neurological Disorders and Stroke
National Institutes of Health
Bethesda, Maryland 20892

Summary

Voltage-activated potassium (K_v) channels contain a central pore domain that is partially surrounded by four voltage-sensing domains. Recent X-ray structures suggest that the two domains lack extensive protein-protein contacts within presumed transmembrane regions, but whether this is the case for functional channels embedded in lipid membranes remains to be tested. We investigated domain interactions in the Shaker K_v channel by systematically mutating the pore domain and assessing tolerance by examining channel maturation, S4 gating charge movement, and channel opening. When mapped onto the X-ray structure of the K_v1.2 channel the large number of permissive mutations support the notion of relatively independent domains, consistent with crystallographic studies. Inspection of the maps also identifies portions of the interface where residues are sensitive to mutation, an external cluster where mutations hinder voltage sensor activation, and an internal cluster where domain interactions between S4 and S5 helices from adjacent subunits appear crucial for the concerted opening transition.

Introduction

Voltage-activated cation channels open and close in response to changes in membrane voltage, a process crucial for their roles in the generation and propagation of electrical signals in the nervous system. The potassium-selective varieties, also known as K_v channels, are tetramers with each subunit containing six transmembrane segments, termed S1–S6. The functional channel complex is comprised of two types of domains or modules: a single pore domain formed by the S5–S6 regions from the four subunits, and four surrounding voltage-sensing domains, each one formed by the S1–S4 segments from a single subunit (Jan and Jan, 1997; Jiang et al., 2003a; Kubo et al., 1993; Li-Smerin and Swartz, 1998; Lu et al., 2001). The pore domain contains the conduction pathway for potassium ions and an activation gate toward the internal side of the membrane that prevents the flow of ions in the closed state (Yellen, 2002). The voltage-sensing domain consists of four or five α helices within the S1–S4 region (Hong and Miller, 2000; Jiang et al., 2003a; Li-Smerin et al., 2000a; Li-Smerin and Swartz, 2001; Long et al., 2005a; Monks et al., 1999) and can be expressed as an isolated domain (Jiang et al., 2003a) or transferred to a non-voltage-gated channel to endow it with voltage sensitivity (Lu et al., 2001, 2002). Similar voltage-sensing domains have recently been identified without an associated pore domain, instead coupled to a soluble phosphatase domain (Murata et al., 2005) or acting as voltage-activated proton channels (Ramsey et al., 2006; Sasaki et al., 2006), which further supports a multidomain architecture within voltage-activated ion channels.

The gating mechanism of the Shaker K_v channel, one of the most extensively studied voltage-activated ion channels, is thought to involve several relatively independent movements of the four voltage-sensing domains between resting (R) and activated (A) states, followed by a concerted opening transition where the S6 gate moves from a closed (C) to an open (O) state. This conceptual model (Scheme 1), taken from the work of Aldrich and coworkers (Ledwell and Aldrich, 1999), is supported by extensive electrophysiological investigation of the wild-type and mutant Shaker K_v channels (Bezanilla et al., 1994; del Camino et al., 2005; Hoshi et al., 1994; Ledwell and Aldrich, 1999; Pathak et al., 2005; Schoppa and Sigworth, 1998a, 1998b, 1998c; Smith-Maxwell et al., 1998a, 1998b; Stefani et al., 1994; Sukhareva et al., 2003; Zagotta et al., 1994a, 1994b).

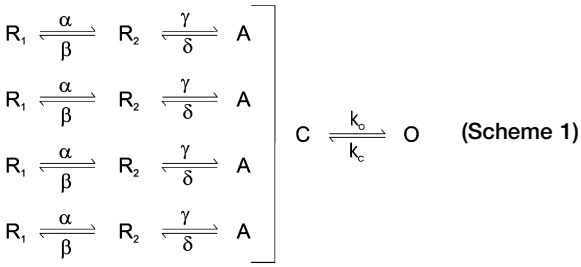

(Scheme 1)

Although movement of the voltage-sensing domains in K_v channels are known to tightly couple to opening and closing of the S6 activation gate (Islas and Sigworth, 1999), the physical basis of this coupling is not established. Both the S4–S5 linker region that connects the pore and voltage-sensing domains (Jiang et al., 2003b; Long et al., 2005b; Lu et al., 2001, 2002; Piper et al., 2005) and the transmembrane interface between domains (Lai et al., 2005; Ledwell and Aldrich, 1999; Li-Smerin et al., 2000b) have been proposed to play important roles in coupling. A specific pairing of the S4–S5 linker with the C-terminal portion of S6 was uncovered in studies where the voltage-sensing domain of Shaker was transplanted onto the KcsA potassium channel (Lu et al., 2001, 2002), highlighting the importance of these regions. The recent crystal structure of the K_v1.2 channel shows tight interactions between the S4–S5 linker and S6, but otherwise suggests that the voltage-sensing and pore domains do not form tight protein-protein

*Correspondence: swartzk@ninds.nih.gov
[2] Present address: Department of Neurobiology, Harvard Medical School, 220 Longwood Avenue, Boston, MA 02115.

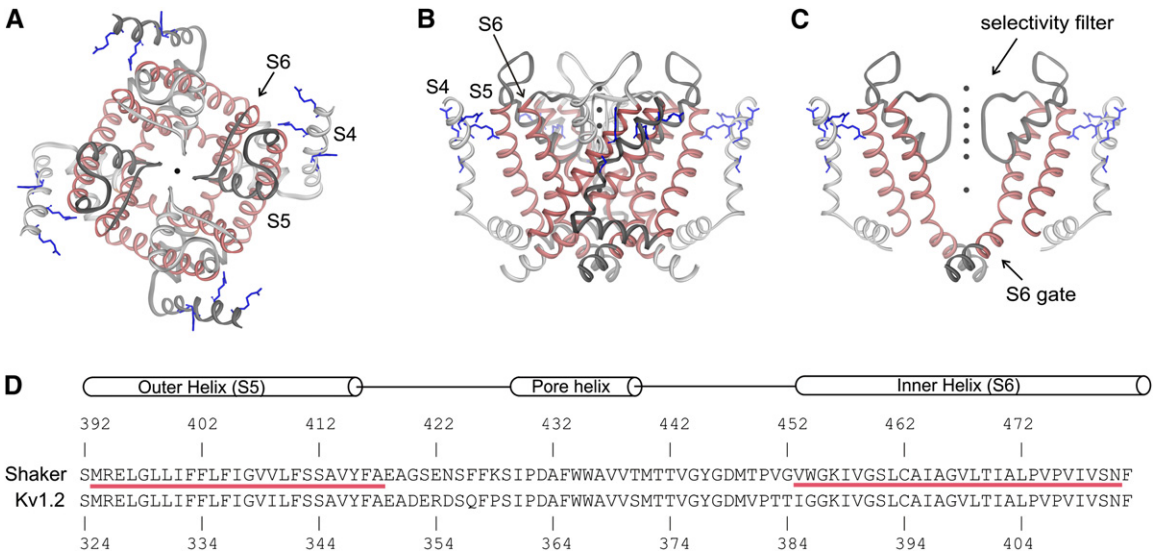

Figure 1. Backbone Fold of the $K_v1.2$ Channel and Sequence Comparison of the Pore Domains in Shaker and $K_v1.2$ Channels

(A) X-ray structure of the S4–S6 region of the $K_v1.2$ channel viewed from an extracellular vantage with mutated regions highlighted in pink and the outer four Arg residues in S4 colored blue. These and all subsequent structures were drawn using DS Viewer Pro 5.0 (Accelrys). PDB Accession Code 2A79. The region from the N terminus through S3 has been omitted.

(B) Side view of the $K_v1.2$ structure.

(C) Same view as in (B), but showing only the S5–S6 region from two subunits and the nearby S4 helix from two adjacent subunits.

(D) Sequence alignment of the Shaker and $K_v1.2$ channels within the pore domain region. Diagram above indicates secondary structural motifs in $K_v1.2$. Residues that were mutated to Trp or Ala in the present study are underlined in pink.

interactions within the plane of the membrane (Jiang et al., 2003b; Long et al., 2005b). In the present study we explore the transmembrane interface between domains for functional channels imbedded in a lipid membrane. We systematically mutated the pore domain of the Shaker K_v channel and then assessed the extent to which mutations are tolerated using measurements of channel maturation, S4 gating charge movement, and channel opening. The results demonstrate that the domain interface tolerates radical mutation quite well and identify a particularly interesting region where interactions between the internal ends of S5 and S4 are important for the concerted open transition.

Results

The objective of the present study is to ascertain whether the transmembrane interface between voltage-sensing and pore domains in the Shaker K_v channel is tightly packed and whether this region serves an important role in coupling movements of the voltage sensors with those in the gate. Two established roles of the S5 and S6 helices within the pore domain of K_v channels are to form a cradle for the selectivity filter toward the extracellular end of the membrane and to form the S6 activation gate at the intracellular end (Figure 1). Mutation of residues that are *exclusively* involved in packing within the pore domain might be expected to disrupt folding of the protein if the packing requirements are rather stringent, or they might alter the concerted opening transition if packing of the residue changes as the intracellular gate region moves. Pore domain residues projecting out toward the voltage-sensing domain might be very sensitive to substitutions of a bulky tryptophan residue if the two domains pack together intimately, or they might be quite tolerant if the two domains have little interaction. The recent crystal structure of the $K_v2.1$ channel (Long et al., 2005a) provides an invaluable structural framework for guiding interpretations because it constrains which residues in S5 and S6 are involved in packing within the pore domain and which are available for interactions with the surrounding voltage sensors. To explore potential interactions between the voltage-sensing and pore domains in the Shaker K_v channel, we mutated each residue in the S5 and S6 helices to tryptophan (Figure 1), expressed the resulting channels in *Xenopus* oocytes, and used voltage-clamp recording techniques to study channel activity. In instances where aromatic residues are present in the wild-type channel, we mutated to alanine. The experiments described below were undertaken to answer two specific questions for each mutant within the pore domain. First, is the mutation so poorly tolerated that it causes retention of the protein in the endoplasmic reticulum (ER) due to misfolding? Second, if the mutant channel traffics to the plasma membrane and remains functional, does the mutation perturb movement of the voltage sensors between R and A states? A substantial perturbation might be expected in regions where the two domains interact if this interaction changes as the voltage sensors activate. To address this second question we measured nonlinear capacitive currents, or gating currents, which result from movement of charged residues as the voltage-sensing domains move between R and A states (Armstrong and Bezanilla, 1973, 1974; Bezanilla and Stefani, 1998; Perozo et al., 1993). To facilitate gating current measurements, most mutants were studied in the background of W434F or V478W (Kitaguchi et al., 2004; Perozo et al., 1993), two mutations that effectively render the

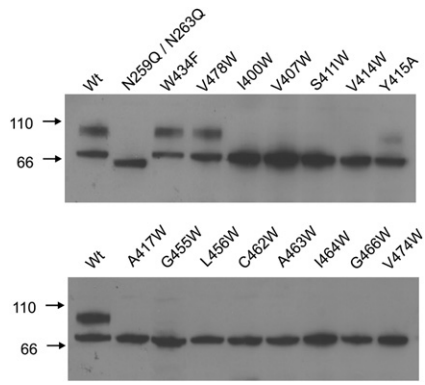

Figure 2. Mutant Shaker K_v Channels with Defects in Maturation

Western blots from SDS poylacrylamide gels of c-*myc*-tagged Shaker protein obtained from crude oocyte membrane preparations. Each lane contains between four to ten oocyte equivalents of Shaker protein. Wild-type protein has two dominant forms, a core glycosylated species (band ~70 kDa) and a more heavily glycosylated mature form (broad band at ~100 kDa). The N259Q/N263Q double mutant shows only a single band at ~65 kDa and marks the position of the unglycosylated protein. Numbers to the left are molecular weight markers in kDa. See Experimental Procedures for details.

channel nonconducting under physiological ionic conditions (see Experimental Procedures). After evaluating perturbations in gating charge movement, we compare these results with previously reported perturbations in opening of the channel (Hackos et al., 2002; Li-Smerin et al., 2000b) to look for domain interactions that might occur during the concerted opening transition.

S5 and S6 Mutants Preventing Maturation

Of the 53 positions mutated, we were able to observe functional activity for mutations at a total of 40 positions. To distinguish whether the remaining 13 mutants disrupt function or are retained in the ER because they are misfolded, we investigated the extent of glycosylation as a marker for retention of mutant Shaker channels in the ER (Papazian et al., 1995; Santacruz-Toloza et al., 1994; Schulteis et al., 1995). Figure 2 shows a Western blot of SDS polyacrylamide gels for wild-type, W434F, V478W, the double mutant N259Q/N263Q, and all 13 mutants in question. The wild-type protein has two dominant forms, a core glycosylated species (band ~70 kDa) that corresponds to the ER-retained fraction and a more heavily glycosylated mature form (broad band at ~100 kDa). The N259Q/N263Q double mutant shows only a single band at ~65 kDa, marking the position of the unglycosylated protein. As expected, W434F and V478W mutants show quantities of mature protein similar to the wild-type channel. However, 12 of the 13 nonfunctional mutants are found in only the core glycosylated form, suggesting that they are retained within the ER. The Y415A mutant seems to behave differently than the other mutants that displayed no electrophysiological activity in that a significant amount of heavily glycosylated protein was detected (Figure 2, last lane of top gel). We are currently exploring this mutant in more detail.

Gating Current Phenotypes for S5 and S6 Mutants

Of the 40 mutants that support functional activity, all but two (S412W and S460W) could be expressed at levels high enough for gating current studies (>10^8 channels per cell). Figure 3 shows gating current records and gating charge (Q) versus voltage (V) relations for the control constructs (W434F or V478W alone) and several of the 38 pore domain mutants for which gating currents could be measured. Some of the mutants display only minor perturbations in charge translocation, as evidenced by Q-V relations that are similar to the controls both in terms of voltage range for charge movement ($V_{1/2}$) and slope (Z). For purposes of categorizing mutations, we

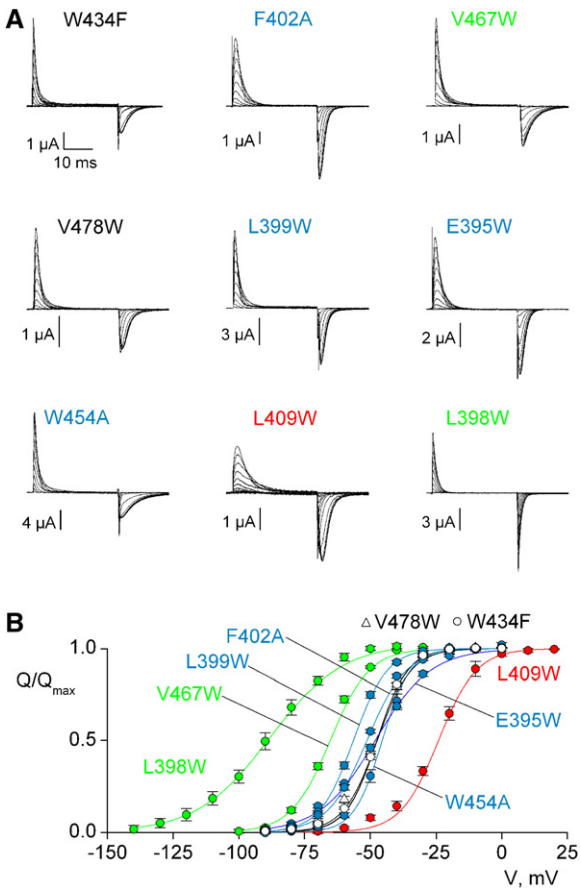

Figure 3. Gating Currents and Q-V Relations for Mutant Shaker K_v Channels

(A) Families of gating current records for W434F, V478W, and seven mutant Shaker channels also containing the W434F mutation. For W434F, E395W, L399W, F402A, V478W, and W454A families, the holding voltage was −90 mV, and depolarizations were to voltages between −90 and 0 mV. For L409W, the holding voltage was −90 mV, and depolarizations were to voltages between −90 and +20 mV. For L398W, the holding voltage was −140 mV and depolarizations to voltages between −140 and −40 mV. For V467W, the holding voltage was −100 mV and depolarizations to voltages between −100 and −40 mV. In all cases, depolarizations were 30 ms in duration and with 10 mV increments between consecutive pulses. The timescale bar shown for W434F applies for all mutants.

(B) Normalized Q-V relations for mutants shown in (A). The control constructs (W434F and V478W) are shown in black. Mutants with Q-V midpoints within 10 mV of controls are shown in blue, with midpoints >10 mV more negative than controls in green and with midpoints >10 mV positive to controls in red. The data points shown are mean ± SEM for gating current measurements made on the same cells listed in Table 1. Smooth curves are simulated Boltzmann functions using mean $V_{1/2}$ and z values listed in Table 1.

Table 1. Gating Properties of Mutant Shaker K_v Channels

Shaker	K_v1.2	Q-V Relation $V_{1/2}$ (mV)	Z	n	Δ $V_{1/2}$ (mV)	G-V Relation $V_{1/2}$ (mV)	Z	Δ $V_{1/2}$ (mV)
Wt						−30.5	3.8	
W434F		−47.6 ± 0.4	4.4 ± 0.1	20				
W434F [a]		−52.3 ± 0.4	4.5 ± 0.1	11				
V478W		−47.5 ± 0.4	4.0 ± 0.1	12				
V478W [a]		−51.8 ± 0.5	3.7 ± 0.04	14				
V478W [b]		−51.3 ± 0.5	3.8 ± 0.02	8				
V478W [c]		−55.3 ± 0.5	3.7 ± 0.1	12				
$M393W_{434}$	M325	−53.8 ± 0.4	4.7 ± 0.1	15	−6.2	−43.9	5.7	−13.4
$R394W_{434}$	R326	−32.1 ± 0.9	3.7 ± 0.5	5	+15.5	−7.2	2.4	+23.3
$E395W_{434}$	E327	−48.3 ± 0.7	2.4 ± 0.1	8	−0.7	+180.4	0.8	+210.9
$L396W_{434}$ [a]	L328	−64.7 ± 0.4	4.8 ± 0.1	6	−12.4			
$G397W_{434}$	G329	−53.7 ± 0.5	4.5 ± 0.1	7	−6.1	−45.3	5.4	−14.8
$L398W_{434}$	L330	−87.3 ± 1.9	1.8 ± 0.1	5	−39.7	+21.1	1.8	+51.6
$L399W_{434}$	L331	−56.5 ± 0.6	3.9 ± 0.1	8	−8.9			
I400W	I332	ERr						
$F401A_{434}$	F333	−56.5 ± 0.3	3.8 ± 0.2	10	−8.9	>+50		>+80
$F402A_{434}$	F334	−51.4 ± 0.4	3.4 ± 0.1	12	−3.8	>+50		>+80
L403W [a]	L335	−68.2 ± 0.6	3.2 ± 0.2	9	−15.9			
$F404A_{434}$	F336	−52.2 ± 0.6	3.9 ± 0.1	8	−4.6	−35.5	4.2	−5.0
$I405W_{434}$	I337	−49.1 ± 0.4	2.4 ± 0.03	15	−1.5	+24.9	2.6	+55.4
$G406W_{478}$	G338	−65.7 ± 0.6	3.1 ± 0.1	11	−18.2	−22.3	2.4	+8.2
V407W	V339	ERr						
$V408W_{434}$ [a]	I340	−29.3 ± 1.1	1.8 ± 0.1	8	+23.0	+2.1	2.3	+32.6
$L409W_{434}$	L341	−24.1 ± 1.1	3.6 ± 0.3	7	+23.5	+1.7	2.5	+32.2
$F410A_{434}$	F342	−40.3 ± 0.8	3.9 ± 0.1	7	+7.3			
S411W	S343	ERr						
$S412W_{434}$	S344	LE						
$S412W_{478}$		LE						
$A413W_{434}$	A345	−29.6 ± 1.7	3.7 ± 0.1	5	+18.0	−18.1	4.2	+12.4
$A413W_{478}$		−25.9 ± 0.9	4.2 ± 0.5	3	+21.6			
V414W	V346	ERr						
Y415A	Y347	§						
$F416A_{434}$	F348	−49.9 ± 0.5	3.5 ± 0.1	8	−2.3	−26.2	2.4	+4.3
A417W	A349	ERr						
$V453W_{434}$	V385	−42.7 ± 0.5	4.2 ± 0.2	3	+4.9	−34.2	4.3	−3.7
$W454A_{434}$	G386	−45.3 ± 0.8	4.9 ± 0.1	6	+2.3	−24.1	2.5	+6.4
G455W	G387	ERr						
K456W	K388	ERr						
$I457W_{434}$ [a]	I389	−39.7 ± 2.0	3.7 ± 0.2	4	+12.6	−13.8	1.9	+16.7
$V458W_{434}$	V390	−28.2 ± 0.8	3.7 ± 0.3	6	+19.4	−6.7	3.3	+24.1
$G459W_{434}$ [a]	G391	−46.7 ± 0.4	4.4 ± 0.3	6	+5.6			
$S460W_{434}$	S392	LE						
$S460W_{478}$		LE						
$L461W_{434}$	L393	−45.6 ± 1.7	4.7 ± 0.1	5	+2.0	−32.2	4.2	−1.7
C462W	C394	ERr						
A463W	A395	ERr						
I464W	I396	ERr						
$A465W_{478}$ [c]	A397	−75.8 ± 0.5	4.0 ± 0.1	6	−20.5	−59.3	8.7	−28.8
G466W	G398	ERr						
$V467W_{434}$	V399	−65.4 ± 0.7	3.5 ± 0.1	8	−17.8			
$L468W_{478}$ [c]	L400	−77.4 ± 0.6	2.8 ± 0.1	12	−22.1	−47.6	4.8	−17.1
$T469W_{434}$	T401	−40.9 ± 0.3	2.6 ± 0.03	10	−6.7	−36.7	5.6	−6.2
$I470W_{434}$	I402	−51.8 ± 0.3	3.9 ± 0.2	8	−4.2	−47.1	7.0	−16.6
$I470W_{478}$ [b]		−56.9 ± 0.4	3.4 ± 0.1	8	−5.1			
$A471W_{434}$	A403	†				−23.8	3.0	+6.7
$L472W_{434}$	L404	−47.9 ± 0.5	3.9 ± 0.3	5	−0.3	+50.4	0.5	+80.9
P473W	P405	−61.9 ± 0.5	3.4 ± 0.1	12	−14.3			
$P473W_{434}$		−62.3 ± 0.4	2.8 ± 0.1	13	−14.7			
V474W	V406	ERr						
$P475W_{434}$	P407	−75.4 ± 0.2	2.4 ± 0.1	7	−27.8			
$V476W_{434}$	V408	−71.9 ± 0.4	5.3 ± 0.1	10	−24.3	−53.4	2.7	−22.9
$I477W_{434}$	I409	−66.5 ± 0.5	4.7 ± 0.2	8	−18.9	−60.4	6.5	−29.9
$S479W_{434}$	S411	−49.7 ± 0.4	2.9 ± 0.04	7	−2.1	+55.0	1.1	+85.5
$N480W_{434}$	N412	−44.6 ± 0.5	3.0 ± 0.1	10	+3.0	+5.3	1.4	+35.8

The first two columns indicate specific mutations made in the Shaker K_v channel and the corresponding residue numbering in the K_v1.2 channel, with subscripts indicating the nonconducting background (either W434F or V478W) used to measure gating currents. Coloring is as follows: blue, $|\Delta V_{1/2}| < 10$ mV; red, $\Delta V_{1/2} > +10$ mV; green, $\Delta V_{1/2} < -10$ mV; orange, ER retained. The midpoint ($V_{1/2}$) and slope (Z) of the Q-V relation, shown as mean ± SEM, are from fits of single Boltzmann functions to data obtained from individual oocytes. $\Delta V_{1/2} = V_{1/2}^{mut} - V_{1/2}^{Wt}$. n represents the number of oocytes in which Q-V relations were obtained with the following exceptions: V478W[b], eight Q-Vs in four cells; $I457W_{434}$, four Q-Vs in three cells; $L472W_{434}$, five Q-Vs in four cells. ERr (ER retained) designates mutants that displayed no detectable ionic or gating currents in either wild-type, W434F, or V478W backgrounds and that failed to show detectable levels of fully glycosylated protein in the maturation assay (see Figure 2). LE (Low-Expression) designates mutants where ionic and gating currents were observed but where the channel could not be expressed to high enough levels for accurate gating current measurements. Data for G-V relations are from Hackos et al., 2002, and Li-Smerin et al., 2000b). $V_{1/2}$ values for F401A and F402A G-V relations are rough estimates only; these mutants display two phases in the voltage-activation relations, with the largest component occurring at very positive voltages and being poorly defined. Values for E395W G-V relations are also approximate as the saturation of the G-V relation is not defined within the voltage range examined. [a]Experiments were done in a Na-free recording solution (see Experimental Procedures). [b]Experiments were done in the standard recording solution plus saturating concentrations of agitoxin-2.

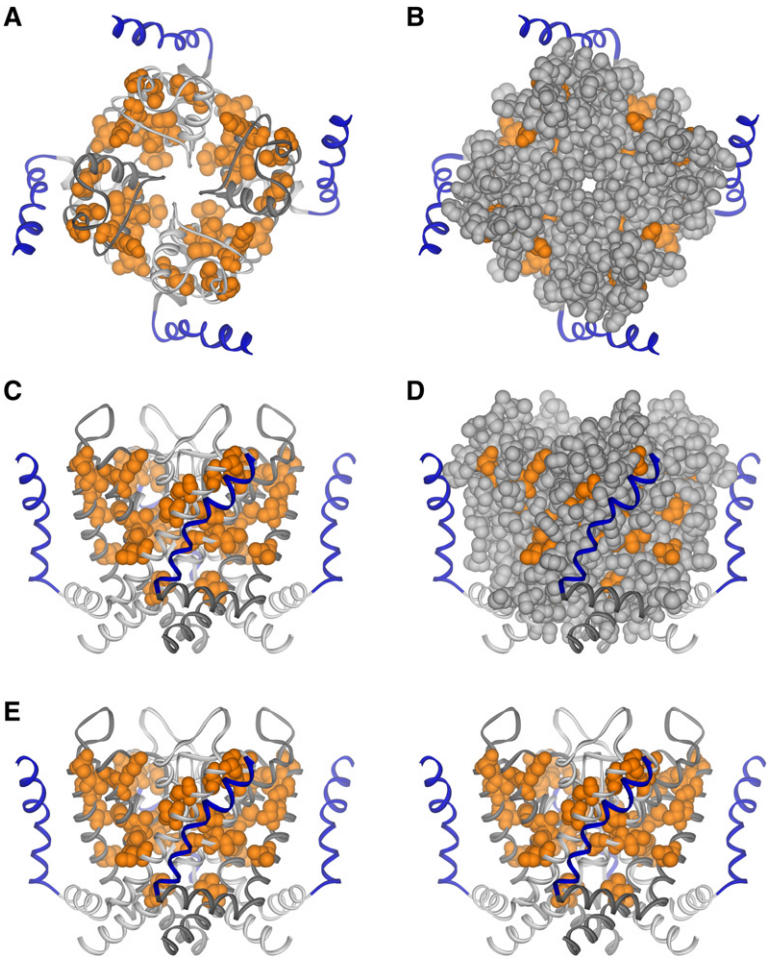

Figure 4. Defects in Maturation Mapped onto the K_v1.2 Structure

(A) Backbone folding model of the S4–S6 region of K_v1.2 viewed from the top. Orange residues (shown as CPK) correspond to the residues in S5 and S6 of Shaker where mutations result in ER retention. The S4 helix is colored blue to highlight its position relative to ER-retained mutations.

(B) Same view as in (A), but with all other residues in the S5–S6 region shown in gray.

(C) Backbone folding model of the S4–S6 region of K_v1.2 viewed from the side colored as in (A).

(D) Same view as in (C), but with all other residues in the S5–S6 region shown in gray.

(E) Stereo pairs of the K_v1.2 structure viewed from the side.

considered a mutation as exhibiting a weak perturbation if the $V_{1/2}$ of the Q-V relation is within 10 mV of the appropriate control construct. A significant number of mutants within S5 and S6 display strong perturbations in gating charge movement, which we operationally defined as having a $V_{1/2}$ shifted by more than 10 mV. One of the most drastic alterations is observed for L398W, a mutant where the $V_{1/2}$ of the Q-V relation is shifted by ~40 mV to more negative voltages and where the slope is decreased to 1.8, rivaling what has been reported for mutations within the S4 helix itself (Aggarwal and MacKinnon, 1996; Perozo et al., 1994; Seoh et al., 1996). Interestingly, a negative shift of the Q-V relation is observed most frequently among mutants producing a strong perturbation (12 out of 18 mutants). L409W is an example of the remaining six mutants exhibiting strong perturbations, where the Q-V relation is shifted toward more positive voltages. Table 1 summarizes the properties of those mutants for which gating current measurements could be obtained.

Mapping of Mutant Phenotypes onto the K_v1.2 Crystal Structure

To evaluate our results, we examined how different mutant phenotypes are distributed within the X-ray structure of the K_v1.2 channel. Figure 4A shows a backbone representation of the S4–S6 region of K_v1.2 X-ray structure, viewed from the extracellular side of the membrane, with orange CPK representation for residues where mutations cause the protein to be retained in the ER. It is evident that most of these residues are located toward the extracellular portion of the protein and that they are either involved in packing between S5 and S6 or interact with residues in the reentrant pore loop that forms the selectivity filter (see also Figures 4B–4D and stereo pairs in Figure 4E and compare with Figure 5). None of the ER-retained mutants project out toward the surrounding S4 helix. The absence of such mutants from the interface between voltage-sensing and pore domains in K_v channels demonstrates the tolerance of this region to mutation, which is

[c]Experiments were done in the Na-free recording solution plus saturating concentrations of agitoxin-2. †It was not possible to hold negative enough to quantitatively define the Q-V relation, but charge movement was observed when depolarizing to −130 mV from a holding potential of −140 mV, indicating a large leftward shift (~40 mV) in the Q-V relationship. §Designates a mutant that displays no detectable ionic or gating currents in either wild-type, W434F, or V478W backgrounds, but where detectable levels of fully glycosylated protein are found in the maturation assay.

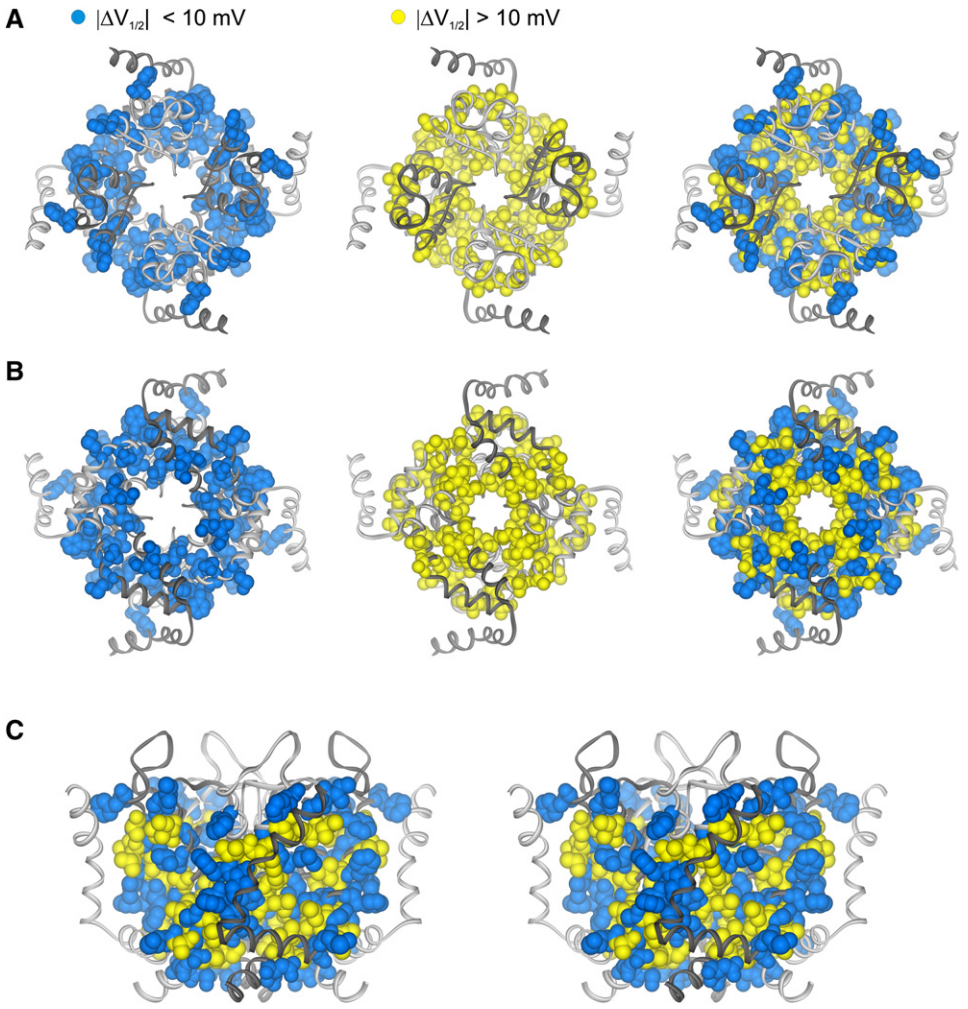

Figure 5. Perturbations in Gating Charge Movement Mapped onto the $K_v1.2$ Structure

(A) Backbone folding models of the S4–S6 region of $K_v1.2$ viewed from the top (outside) with residues where mutations only weakly perturb the Q-V relation ($|\Delta V_{1/2}| < 10$ mV) colored blue (shown as CPK) and those strongly perturbing the Q-V relation ($|\Delta V_{1/2}| > 10$ mV) colored yellow. $\Delta V_{1/2} = V_{1/2}^{mut} - V_{1/2}^{Wt}$.

(B) View from the bottom (inside) colored as in (A).

(C) Stereo pairs of the $K_v1.2$ structure viewed from the side with coloring as in (A).

consistent with the presence of a rather unconstrained interface between domains.

We next mapped our results from the functional characterization of gating current phenotypes onto the $K_v1.2$ structure, initially only considering whether a mutant produces a weak or strong perturbation in the Q-V (Figure 5). If the interface between voltage-sensing and pore domains involves extensive interactions, we might expect residues on the perimeter of the pore domain to exhibit particularly strong perturbations in gating charge movement. Remarkably, the mutants producing strong perturbations (yellow residues) are not concentrated on the perimeter of the pore domain but are found throughout both S5 and S6 helices. Many of the 20 weakly perturbing mutants (blue residues) are positioned at the periphery of the pore domains, and if anything, strong perturbations tend to be concentrated within the core of the pore domain (Figure 5).

The strongly perturbing mutants that are located at the interface between the voltage-sensing and pore domains in the $K_v1.2$ structure are clustered together near the external side of the membrane. Mutations in this region, which we term the "external cluster," can be seen to shift the Q-V toward positive voltages and thus perturb the equilibrium between R and A states of the voltage sensor in favor of the R state (red residues in Figure 6). When the time constant for decay of the On gating current is plotted as a function of voltage, most of the mutants in the external cluster show a pronounced slowing at positive voltages (Figure 6D), suggesting that the rate of voltage sensor activation is slowed. Although channel opening for each of the mutants in the external cluster is also shifted toward positive membrane voltages (Table 1), the $K_v1.2$ structure suggests that these residues are not positioned where they might directly influence the dynamics of the S6

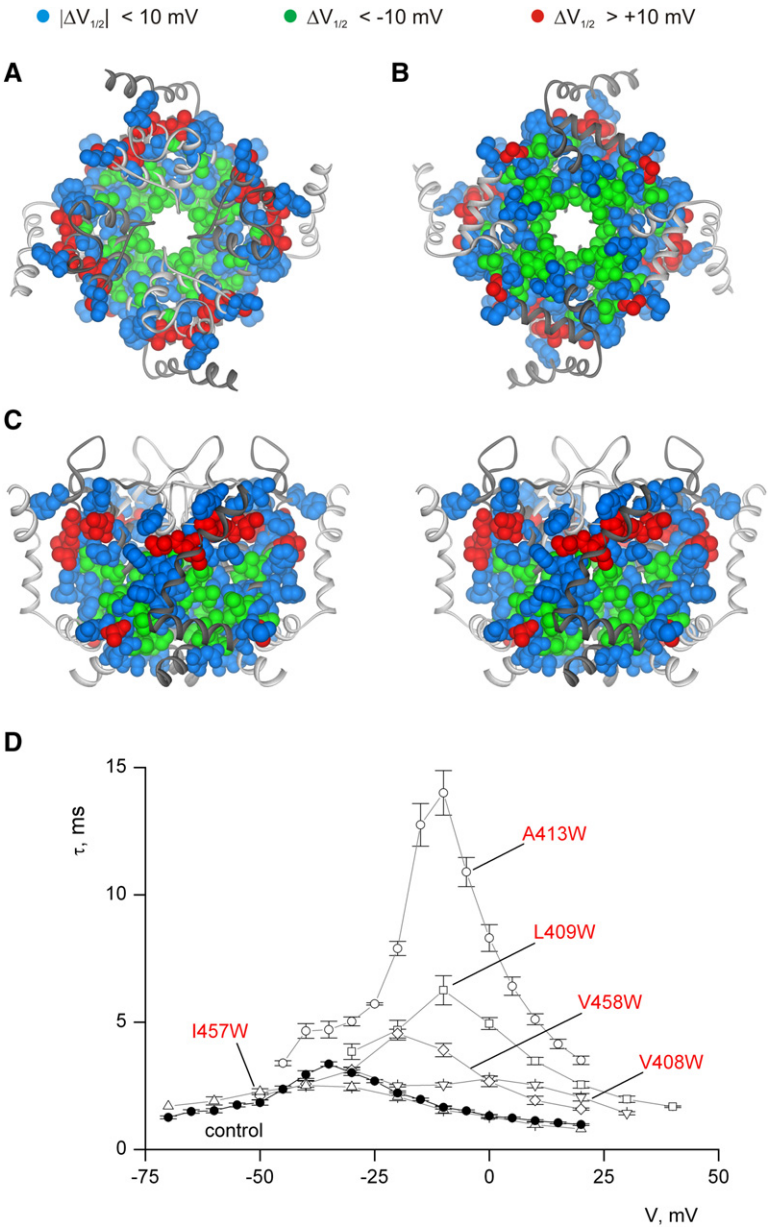

Figure 6. Distribution of Mutants Favoring Resting and Activated Voltage Sensors

(A) Backbone folding model of the S4–S6 region of $K_v1.2$ viewed from the top (outside) with residues where mutations strongly perturb the Q-V relation in favor of the resting voltage sensors colored red (shown as CPK). Blue residues are weakly perturbing and green residues are strongly perturbing in favor of voltage sensor activation. $\Delta V_{1/2} = V_{1/2}^{mut} - V_{1/2}^{Wt}$.

(B) View from the bottom (inside) colored as in (A).

(C) Stereo pairs of the $K_v1.2$ structure viewed from the side with coloring as in (A).

(D) Plot of time constant (τ) for On gating current relaxations against test voltage (V) for control (W434F) and mutants shifting the Q-V toward positive voltages. On gating current relaxations were fit with a single exponential function for each test voltage. Data points are mean ± SEM. All mutants were studied with the W434F background. n = 11 for control (W434F), 8 for V408W, 7 for L409W, 4 for A413W, 6 for I457W, and 5 for V458W.

gate, indicating that these mutations influence the equilibrium and dynamics of the voltage sensors proper.

A Cluster of Mutants Affecting the Concerted Opening Transition

The results discussed thus far show that mutations at the interface between voltage-sensing and pore domains do not disrupt folding of the channel protein and with the exception of the external cluster do not have dramatic effects on movements of the voltage sensors between R and A states. Keeping in mind that the present mutations involve rather dramatic changes in side chain volume and chemistry, involving substitution of a bulky tryptophan or a quite small alanine, these results support the notion of a relatively unconstrained transmembrane interface between the two domains for the early steps in Scheme 1. To explore domain interactions that may be important for the later concerted opening transition, we compared the effects of mutants on Q-V relations and channel opening. Conductance-voltage (G-V) relations are available from previous studies (Hackos et al., 2002; Li-Smerin et al., 2000b) for many of the mutants studied here, and the $V_{1/2}$ and Z values obtained by fitting single Boltzmann functions to those relations are listed in Table 1. Plotting of the $V_{1/2}$ for G-V relations against that for Q-V relations reveals three primary groups of mutants (Figure 7). Those in the external cluster exhibit Q-V and G-V relations that are similarly shifted to positive voltages (Figure 7; top right quadrant), which makes sense if the primary effect of the mutants are on voltage sensor activation. Another group of mutants, primarily those within the S6 region of the channel, exhibit Q-V and G-V relations that are similarly shifted to negative voltages (Figure 7; lower left quadrant). Here the effect of the mutation is probably to destabilize the closed state of the gate as these residues are involved in the packing

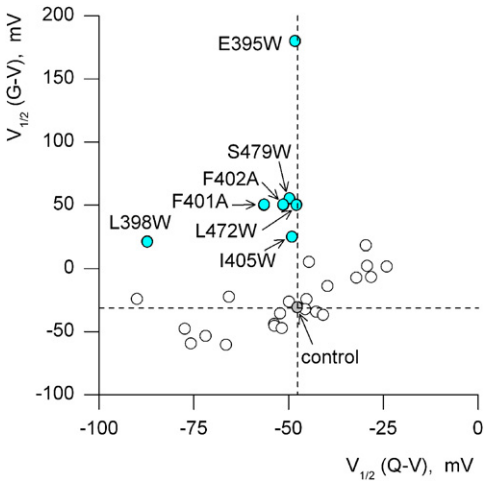

Figure 7. Relationship between Midpoints of G-V and Q-V Relations

Midpoints ($V_{1/2}$) were obtained by fitting Q-V and G-V relations with single Boltzmann functions (see Table 1). $V_{1/2}$ values for F401A and F402A G-V relations are approximate; these mutants display two phases in the voltage-activation relations, with the largest component occurring at very positive voltages and being poorly defined (see Figure 8).

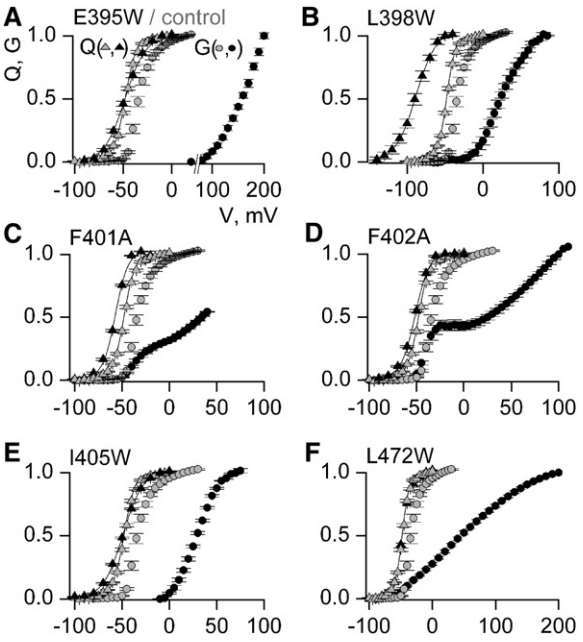

Figure 8. Mutants Perturbing the Concerted Opening Transition

(A) Gating charge (Q; triangles) and macroscopic conductance (G; circles) plotted against membrane voltage (V) for control (gray) and E395W (black). n = 7 and 3 for control and E395W G-Vs, respectively.
(B) Q-V and G-V data for L398W (black). n = 5 for L398W G-Vs.
(C) Q-V and G-V data for F401A (black). n = 5 for F401A G-Vs.
(D) Q-V and G-V data for F402A (black). n = 3 for F402A G-Vs.
(E) Q-V and G-V data for I405W (black). n = 3 for I405W G-Vs.
(F) Q-V and G-V data for L472W (black). n = 6 for L472W G-Vs. For all Q-Vs and G-Vs, data points are mean ± SEM and were normalized to the value available at the most positive voltage shown. For all Q-Vs, n is shown in Table 1, smooth curves are simulated Boltzmann functions using mean $V_{1/2}$ and Z values listed in Table 1, and all mutants were studied with the W434F background.

within the S6 gate region (Hackos et al., 2002; Yifrach and MacKinnon, 2002). The shift of the Q-V to negative voltages is probably best explained by the fact that charge movement through open channels occurs at more negative voltages compared to closed channels (Horrigan and Aldrich, 2002). The final group of mutants is unique in that their Q-V relations exhibit small to dramatic shifts toward negative voltages while their G-V relations display pronounced shifts in the opposite direction (Figure 7; upper left quadrant; Figure 8), and all are located within the internal half of the channel protein. This group of mutants, which we term the "internal cluster," includes E395W, L398W, F401A, F402A, and I405W in the S5 helix and both L472W and S479W in the S6 helix, and all exhibit concerted opening transitions that are dramatically perturbed in favor of the closed state (Figures 7 and 8). The F401A and F402A mutants are additionally unique in that they have two distinct phases in the G-V relation, one that occurs in a similar voltage range to the wild-type channel and another at greatly depolarized voltages (Figure 8). The collective data for mutants within the internal cluster suggest that movement of the voltage sensors between resting and activated states is weakly to strongly perturbed in favor of activation, whereas the concerted opening transition is strongly perturbed in favor of the closed state, as if a critical link between conformational changes in the voltage sensors and the gate has been altered. None of the residues within the internal cluster are involved in packing between the S5 and S6 helices (Figure 9; turquoise residues), where such dramatic effects on the concerted opening transition might in principle be expected. Instead, residues within the internal cluster form a relatively well-defined and continuous patch in the structure of $K_v1.2$, spanning from roughly the middle to the intracellular end of the membrane. L398, F401, F402, and I405 in particular project directly out toward the nearby S4 helix from the adjacent subunit, suggesting that the internal cluster demarcates a region where domain interactions are crucial for the concerted opening transition.

Discussion

The primary objective of the present study is to investigate whether a functionally significant transmembrane protein-protein interface exists between the voltage-sensing and pore domains in the Shaker K_v channel. If these domains pack together tightly, we might expect that mutations on the pore domain side would perturb charge-translocating movements within the voltage sensors. Although we made quite radical mutations throughout both the S5 and S6 helices, the general impression is that the mutation of residues positioned physically nearest the voltage sensors do not elicit very substantial perturbations in voltage sensor activation. This point is evident when comparing the weakly and strongly perturbing mutations (Figure 5), with the former being somewhat more concentrated toward the periphery of the pore domain and the latter within regions involved in packing of the S6 gate. The distribution of mutants that prevent maturation of the channel provide a strong impression that the domain interface is rather tolerant; many such mutants can be found within the packing between S5, S6, and the selectivity filter, but

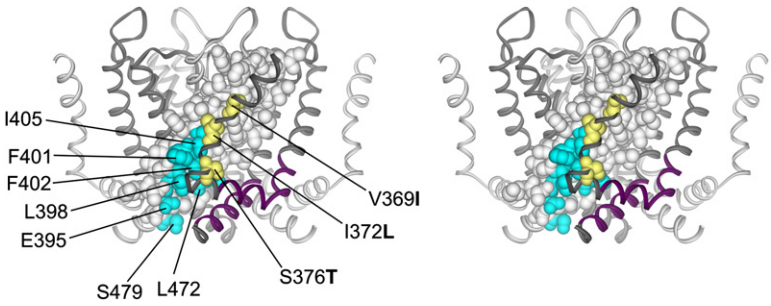

Figure 9. Distribution of Mutants Perturbing the Concerted Opening Transition

Stereo pairs of the S4–S6 region of the $K_v1.2$ structure viewed from the side. Residues where mutations have profound effects on the concerted opening transition (see Figures 7 and 8) colored turquoise (shown as CPK). Numbers correspond to those in the Shaker K_v channel. Mutant residues in the ILT triple mutant are colored yellow (shown as CPK), and the interaction between the S4–S5 linker (317–331 in $K_v1.2$) and S6 (405–417 in $K_v1.2$) defined by Lu and colleagues (Lu et al., 2001, 2002) colored purple in the adjacent subunit.

not between the voltage-sensing and pore domains (Figures 2 and 4). Taken together, these results suggest that much of the transmembrane interface between voltage-sensing and pore domains is relatively unconstrained, consistent with the absence of tight packing that is observed in crystal structures of the K_vAP and $K_v1.2$ channels (Jiang et al., 2003b; Long et al., 2005b).

Although much of the domain interface appears loosely packed, functionally significant perturbations do occur in two regions, arguing against the possibility that the voltage-sensing domains simply float like buoys in the membrane. The first is the external cluster where mutations shift the Q-V relation to more depolarized voltages (Figure 6; red residues) and slow activation of the voltage sensors (Figure 6D). Metal bridging studies in Shaker (Laine et al., 2003) and the structure of $K_v1.2$ (Long et al., 2005a) suggest that the extracellular end of S4 is positioned close to residues within this cluster, supporting the possibility that perturbations within the external cluster result from a local interaction with S4. All of the residues in the external cluster are hydrophobic (V408, L409, A413, I457, and V458) and in each case the mutations to tryptophan result in a substantial increase in side chain volume (39–96 $Å^3$), raising the possibility that the interaction here has been created by the mutation and may not be energetically important in the wt channel. One possibility is that these perturbations result from a steric interaction between domains that retards voltage sensor activation. Another possibility is that mutations of aliphatic residues within the external cluster disrupt the interaction of channel domains with lipids that might serve to prevent side chain interactions across domains in this region. The importance of non-annular lipid interactions with membrane proteins is becoming increasingly appreciated (Lee, 2003, 2004), and lipid modifications within the external leaflet have pronounced effects on voltage sensor activation (Ramu et al., 2006), raising the possibility that lipids interact in a relatively specific manner with regions of K_v channels involved in gating.

The most interesting region that our results identify is the internal cluster of channel residues located at the interface between the voltage-sensing and pore domains, where mutations have pronounced effects on the concerted opening transition (Figures 7 and 8). Mutants in this region (E395W, L398W, F401A, F402A, I405W, L472W, and S479W) produce mild to strong perturbations that favor the activated voltage sensor while dramatically favoring the closed state of the S6 gate (Figures 7 and 8). The phenotype of the L398W mutant is the most pronounced example within this cluster, with the Q-V shifting by about −40 mV and the G-V by over +50 mV. Previous studies (Kanevsky and Aldrich, 1999) have shown that the F401A mutant in this cluster alters the C-O transition by greatly increasing the closing rate (k_c in Scheme 1), suggesting that the effect on opening results from a profound destabilization of the open state. The phenotypes observed within this concerted opening cluster would be consistent with an interaction between the voltage-sensing and pore domains that is particularly important during the concerted opening transition. These residues are not involved in the packing between S5 and S6 (Figure 9; turquoise residues), where such dramatic effects on the concerted opening transition might be explained by effects on the intrinsic stability of either closed or open states of the gate. Instead, these residues cluster together, and many of them, most notably L398, F401, F402, and I405, project out toward the nearby S4 helix from the adjacent subunit. The perturbations observed here are unlikely to result from an interaction that is introduced by the mutation alone because similar phenotypes are observed regardless of whether aromatic phenylalanine residues were mutated to alanine (e.g., F401, F402) or sizable leucine and isoleucine residues were mutated to tryptophan (e.g., L398, I405). The possibility of a direct interaction between this region of S5 with the internal half of S4 is strengthened by the similarity of the phenotype for the concerted opening cluster to that of the ILT triple mutant within the S4 of Shaker (V369I, I372L, and S376T), which also has pronounced effects on the concerted opening transition (Ledwell and Aldrich, 1999; Smith-Maxwell et al., 1998a, 1998b). Remarkably, the internal cluster is positioned to directly interact with the ILT residues in S4 (Figure 9; yellow residues). The physical proximity and phenotypical similarity between those residues in the voltage-sensing and pore domains strongly suggest that the interactions between the two groups of residues most likely underlie the concerted transition leading to the channel opening.

The internal cluster is particularly interesting when considered in the context of the emerging picture that gating of K_v channels involves two distinct types of voltage sensor movement. The first motion results in the bulk of the gating charge movement detected from gating current measurements and corresponds to the movement of the four voltage sensors between R and A states (Bezanilla et al., 1994; Hoshi et al., 1994; Ledwell and Aldrich, 1999; Pathak et al., 2005; Perozo et al., 1994;

Schoppa and Sigworth, 1998a, 1998b, 1998c; Smith-Maxwell et al., 1998a, 1998b; Stefani et al., 1994; Zagotta et al., 1994a, 1994b). This early motion occurs relatively independently in the four subunits (Ding and Horn, 2001; Horn et al., 2000; Mannuzzu and Isacoff, 2000; Schoppa and Sigworth, 1998c; Smith-Maxwell et al., 1998a; Zagotta et al., 1994a) and results in a detectable change in chemical accessibility in the vicinity of the S6 gate but does not actually open the gate (del Camino et al., 2005; Pathak et al., 2005). A dearth of rigid constraints between voltage-sensing and pore domains, a notion supported by several K_v channel structures (Jiang et al., 2003a; Lee et al., 2005; Long et al., 2005a) and the present work, would allow this first type of voltage sensor movement to occur without causing distributed structural changes within the pore domains. There is also evidence for a second type of voltage sensor motion during the concerted opening transition that involves the movement of only a small amount of gating charge (del Camino et al., 2005; Mannuzzu and Isacoff, 2000; Pathak et al., 2005; Schoppa and Sigworth, 1998c; Smith-Maxwell et al., 1998a, 1998b; Zagotta et al., 1994a). One intriguing possibility is that the internal cluster demarcates a region where interactions between the voltage sensors and the pore domain enable the second type of voltage sensor motion to open the S6 gate. The marked speeding of channel closing observed in the F401A mutant (Kanevsky and Aldrich, 1999) would fit with an interaction between an activated S4 and the hydrophobic residues in the concerted opening cluster that stabilize the gate in an open conformation. Disruption of this interaction might actually allow the gate to slip shut even though the voltage sensors remain activated. The $K_v1.2$ structure is consistent with an intersubunit interaction between this cluster and the S4 helix from the adjacent subunit, which makes this interaction particularly attractive for playing an important role in the concerted opening of the gate. The previously identified interaction between the S4–S5 linker and S6 helices that is necessary for imparting voltage sensitivity to KcsA (Lu et al., 2001, 2002), is predicted from the $K_v1.2$ structure to largely occur within a single subunit (Figure 9; purple helical regions). One possibility is that the intrasubunit S4–S5 linker to S6 interaction serves a general role in allowing the S6 gate to follow S4 motions and that the S4 to S5 intersubunit interaction serves a more specific role in coupling the second S4 motion to the final concerted opening transition.

Experimental Procedures

Molecular Biology and Channel Expression

All experiments were performed using the Shaker H4 K_v channel (Kamb et al., 1988) with a deletion of residues 6–46 to remove fast inactivation (Hoshi et al., 1990; Zagotta et al., 1990). Point mutations in Shaker, either in pBlu-SK+ or pGEM-HE (Liman et al., 1992), were generated through sequential PCR, ligation into appropriately digested vectors, and their sequence verified by automated DNA sequencing. All cDNA constructs were linearized with HindIII (bluescript) or NheI (pGEM-HE) and transcribed using T7 RNA polymerase. *Xenopus laevis* oocytes were removed surgically and incubated with agitation for 1–1.5 hr in a solution containing (in mM) 82.5 NaCl, 2.5 KCl, 1 $MgCl_2$, 5 HEPES, and 2 mg/ml collagenase (Worthington Biochemical Corp.), pH 7.6 with NaOH. Defolliculated oocytes were injected with cRNA and incubated at 17°C in a solution containing (in mM) 96 NaCl, 2 KCl, 1 $MgCl_2$, 1.8 $CaCl_2$, 5 HEPES, and 50 μg/ml gentamicin (Invitrogen/GIBCO BRL), pH 7.6 with NaOH for 1–7 days before electrophysiological recording or harvesting of channel protein.

Examination of Channel Maturation

The extent of glycosylation (at Asn259 and Asn263) was determined to assess whether selected mutants are retained in the endoplasmic reticulum (Papazian et al., 1995; Santacruz-Toloza et al., 1994; Schulteis et al., 1995). In order to detect Shaker protein for the maturation assay, a tagged Shaker construct was generated that contained c-*myc* epitopes (Glu-Gln-Lys-Leu-Ile-Ser-Glu-Glu-Asp-Leu) inserted at the N terminus (after Ala5) and the C terminus (after Val638). In addition, a sequence encoding for Arg, Gly, Ser, and 6 His residues was inserted at the C terminus immediately after the c-*myc* epitope. Four days after cRNA injection, a crude membrane fraction was harvested from oocytes using previously described procedures (Kobertz et al., 2000). Briefly, batches of 30 to 40 oocytes were homogenized in 1 ml of HEDP buffer (100 mM HEPES, 1 mM EDTA, pH 7.6 with NaOH) plus the following cocktail of protease inhibitors: 0.5 mM PMSF (Sigma), 50 μg/ml antipain (Sigma), 25 μg/ml (4-amidinophenyl) methanesulfonyl fluoride (Sigma), 40 μg/ml bestatin (Sigma), 4 TIU/ml aprotinin (ICN), 0.5 μg/ml leupeptin (Sigma), 0.7 μg/ml pepstatin A (Sigma). Homogenization and all subsequent steps were performed at 4°C. Oocyte homogenates in HEDP buffer were centrifuged at 3000 × g for 10 min. The supernatant was then overlaid on a 15% sucrose cushion prepared in ice-cold HEDP buffer and centrifuged at 175,000 × g for 1.5 hr. The crude membrane pellet was then solubilized in NuPAGE LDS sample buffer (Invitrogen) with 50 mM DTT and subjected to electrophoresis and Western analysis. Samples (each consisting of ~4 to 10 oocytes equivalents of protein) were heated to 70°C for 10 min and loaded onto 10% Nu-PAGE Bis-Tris gel (Invitrogen) using the following solution as running buffer: 50 mM MOPS, 50 mM Tris base, 3.46 mM SDS, and 1 mM EDTA. See Blue Plus 2 (Invitrogen) was used as the protein molecular weight marker. Protein in the gel was then transferred onto nitrocellulose membrane (Amersham Pharmacia) using a semidry electrotransfer apparatus (E and K Scientific Products) where the transfer buffer consisted of 25 mM bicine, 25 mM bis-tris, 1 mM EDTA, and 10% methanol. After probing the nitrocellulose membrane with mouse anti-myc antibody (Invitrogen), protein expression was detected using ECL Western blotting detection reagents (Amersham Pharmacia).

Measurement of Gating Currents

To facilitate gating current measurements, most S5 and S6 mutations were examined in the background of W434F, a mutation that effectively renders the channel nonconducting in the presence of K^+ and thus enabling gating current measurements without significant interference from ionic currents (Perozo et al., 1993; Starkus et al., 1998; Yang et al., 1997). Two mutants (P473W and V478W) give rise to nonconducting channels in the absence of W434F (Hackos et al., 2002; Li-Smerin et al., 2000b). In the case of L403W, gating currents can be studied without W434F because voltage sensor movement and activation occur over different voltage ranges. Several S5 and S6 mutants (G406W, A465W, L468W, and I470W) were found to rescue ion conduction in the W434F mutant background. Although the pore-blocking toxin agitoxin-2 (Garcia et al., 1994) can be used to isolate gating currents from ionic currents, the toxin does not inhibit ion conduction in the W434F background (presumably because it does not bind to the W434F mutant). We therefore examined these mutations in V478W, another nonconducting mutant that retains sensitivity to agitoxin-2 and exhibits a Q-V relationship similar to W434F (Table 1 and Figure 3) (Hackos et al., 2002; Kitaguchi et al., 2004). Although G406W, A465W, L468W, and I470W also rescued ion conduction in the V478W background, gating current measurements could be obtained for these mutants in the presence of the toxin. In Table 1 the identity of the background mutant is indicated by a subscript following the identity of the primary mutation under examination.

Gating currents were measured using two-electrode voltage-clamp recording techniques (Oocyte clamp model OC-725C; Warner Instruments) with low resistance (~0.1–0.3 MΩ) current injection electrodes. In most instances, oocytes were perfused in a 160 μl recording chamber with a standard extracellular solution containing (in mM) 100 NaCl, 2 KCl, 1 $MgCl_2$, 0.3 CaCl, and 15 HEPES, pH 7.6. In some instances (see Table 1) experiments were carried out with

a Na-free solution that contained 100 mM N-Methyl-D-Glucamine (NMDG) in place of NaCl. For mutants that diplayed ionic current in the V478W background, recordings were obtained in the presence of saturating concentrations (1–10 μM) of agitoxin-2 (Alomone labs). Data were filtered at 2 kHz (eight-pole Bessel) and digitized at 10 kHz. Microelectrodes were filled with 3 M KCl and had resistances between 0.1 and 0.6 MΩ. All experiments were conducted at room temperature (~22°C). Gating currents were elicited by 30 ms depolarization to various test voltages and subsequent repolarization to the holding voltage. Holding voltages ranged from −90 mV to −140 mV and were chosen so that no significant charge movement could be detected by a 10 mV depolarizing pulse. Linear capacity and background currents were subtracted using a P/-4 protocol (Armstrong and Bezanilla, 1974).

Q-V relations were fit with single Boltzmann functions (e.g., Figure 3) according to:

$$Q/Q_{max} = \left(1 + e^{-ZF(V - V_{1/2})/RT}\right)^{-1}$$

where Q/Q_{max} is the normalized charge obtained by integrating the ON and OFF components of the gating currents, Z is the equivalent charge, $V_{1/2}$ is the half-activation voltage, F is Faraday's constant, R is the gas constant, and T is temperature in Kelvin.

The G-V relations shown in Figure 8 were obtained by measuring tail currents or steady-state outward K^+ currents (I) following a series of membrane depolarizations; in the latter instance, G was calculated according to $G = I/(V - V_{rev})$. The extracellular recording solution for measuring ionic currents contained (in mM) RbCl (50), NaCl (50), $MgCl_2$ (1), $CaCl_2$ (0.3), HEPES (5), pH 7.6 with NaOH.

Acknowledgments

We thank Miguel Holmgren, Joe Mindell, Revell Phillips, and Shai Silberberg for helpful discussions and J. Nagle and D. Kauffman in the NINDS DNA sequencing facility for sequencing mutant constructs. This work was supported by the Intramural Research Program of the NINDS, NIH.

Received: July 27, 2006
Revised: October 4, 2006
Accepted: October 9, 2006
Published: November 21, 2006

References

Aggarwal, S.K., and MacKinnon, R. (1996). Contribution of the S4 segment to gating charge in the Shaker K^+ channel. Neuron *16*, 1169–1177.

Armstrong, C.M., and Bezanilla, F. (1973). Currents related to movement of the gating particles of the sodium channels. Nature *242*, 459–461.

Armstrong, C.M., and Bezanilla, F. (1974). Charge movement associated with the opening and closing of the activation gates of the Na channels. J. Gen. Physiol. *63*, 533–552.

Bezanilla, F., and Stefani, E. (1998). Gating currents. Methods Enzymol. *293*, 331–352.

Bezanilla, F., Perozo, E., and Stefani, E. (1994). Gating of Shaker K^+ channels: II. The components of gating currents and a model of channel activation. Biophys. J. *66*, 1011–1021.

del Camino, D., Kanevsky, M., and Yellen, G. (2005). Status of the intracellular gate in the activated-not-open state of shaker K^+ channels. J. Gen. Physiol. *126*, 419–428.

Ding, S., and Horn, R. (2001). Slow photo-cross-linking kinetics of benzophenone-labeled voltage sensors of ion channels. Biochemistry *40*, 10707–10716.

Garcia, M.L., Garcia-Calvo, M., Hidalgo, P., Lee, A., and MacKinnon, R. (1994). Purification and characterization of three inhibitors of voltage- dependent K^+ channels from Leiurus quinquestriatus var. hebraeus venom. Biochemistry *33*, 6834–6839.

Hackos, D.H., Chang, T.H., and Swartz, K.J. (2002). Scanning the intracellular s6 activation gate in the shaker K^+ channel. J. Gen. Physiol. *119*, 521–532.

Hong, K.H., and Miller, C. (2000). The lipid-protein interface of a Shaker K^+ channel. J. Gen. Physiol. *115*, 51–58.

Horn, R., Ding, S., and Gruber, H.J. (2000). Immobilizing the moving parts of voltage-gated ion channels. J. Gen. Physiol. *116*, 461–476.

Horrigan, F.T., and Aldrich, R.W. (2002). Coupling between voltage sensor activation, Ca^{2+} binding and channel opening in large conductance (BK) potassium channels. J. Gen. Physiol. *120*, 267–305.

Hoshi, T., Zagotta, W.N., and Aldrich, R.W. (1990). Biophysical and molecular mechanisms of Shaker potassium channel inactivation. Science *250*, 533–538.

Hoshi, T., Zagotta, W.N., and Aldrich, R.W. (1994). Shaker potassium channel gating. I: Transitions near the open state. J. Gen. Physiol. *103*, 249–278.

Islas, L.D., and Sigworth, F.J. (1999). Voltage sensitivity and gating charge in Shaker and Shab family potassium channels. J. Gen. Physiol. *114*, 723–741.

Jan, L.Y., and Jan, Y.N. (1997). Voltage-gated and inwardly rectifying potassium channels. J. Physiol. *505*, 267–282.

Jiang, Y., Lee, A., Chen, J., Ruta, V., Cadene, M., Chait, B.T., and MacKinnon, R. (2003a). X-ray structure of a voltage-dependent K^+ channel. Nature *423*, 33–41.

Jiang, Y., Ruta, V., Chen, J., Lee, A., and MacKinnon, R. (2003b). The principle of gating charge movement in a voltage-dependent K^+ channel. Nature *423*, 42–48.

Kamb, A., Tseng-Crank, J., and Tanouye, M.A. (1988). Multiple products of the Drosophila Shaker gene may contribute to potassium channel diversity. Neuron *1*, 421–430.

Kanevsky, M., and Aldrich, R.W. (1999). Determinants of voltage-dependent gating and open-state stability in the S5 segment of Shaker potassium channels. J. Gen. Physiol. *114*, 215–242.

Kitaguchi, T., Sukhareva, M., and Swartz, K.J. (2004). Stabilizing the closed S6 gate in the Shaker Kv channel through modification of a hydrophobic seal. J. Gen. Physiol. *124*, 319–332.

Kobertz, W.R., Williams, C., and Miller, C. (2000). Hanging gondola structure of the T1 domain in a voltage-gated K^+ channel. Biochemistry *39*, 10347–10352.

Kubo, Y., Baldwin, T.J., Jan, Y.N., and Jan, L.Y. (1993). Primary structure and functional expression of a mouse inward rectifier potassium channel. Nature *362*, 127–133.

Lai, H.C., Grabe, M., Jan, Y.N., and Jan, L.Y. (2005). The S4 voltage sensor packs against the pore domain in the KAT1 voltage-gated potassium channel. Neuron *47*, 395–406.

Laine, M., Lin, M.C., Bannister, J.P., Silverman, W.R., Mock, A.F., Roux, B., and Papazian, D.M. (2003). Atomic proximity between S4 segment and pore domain in Shaker potassium channels. Neuron *39*, 467–481.

Ledwell, J.L., and Aldrich, R.W. (1999). Mutations in the S4 region isolate the final voltage-dependent cooperative step in potassium channel activation. J. Gen. Physiol. *113*, 389–414.

Lee, A.G. (2003). Lipid-protein interactions in biological membranes: a structural perspective. Biochim. Biophys. Acta *1612*, 1–40.

Lee, A.G. (2004). How lipids affect the activities of integral membrane proteins. Biochim. Biophys. Acta *1666*, 62–87.

Lee, S.Y., Lee, A., Chen, J., and Mackinnon, R. (2005). Structure of the KvAP voltage-dependent K+ channel and its dependence on the lipid membrane. Proc. Natl. Acad. Sci. USA *102*, 15441–15446.

Li-Smerin, Y., and Swartz, K.J. (1998). Gating modifier toxins reveal a conserved structural motif in voltage-gated Ca^{2+} and K^+ channels. Proc. Natl. Acad. Sci. USA *95*, 8585–8589.

Li-Smerin, Y., and Swartz, K.J. (2001). Helical structure of the COOH terminus of S3 and its contribution to the gating modifier toxin receptor in voltage-gated ion channels. J. Gen. Physiol. *117*, 205–218.

Li-Smerin, Y., Hackos, D.H., and Swartz, K.J. (2000a). Alpha-helical structural elements within the voltage-sensing domains of a K^+ channel. J. Gen. Physiol. *115*, 33–49.

Li-Smerin, Y., Hackos, D.H., and Swartz, K.J. (2000b). A localized interaction surface for voltage-sensing domains on the pore domain of a K^+ channel. Neuron *25*, 411–423.

Liman, E.R., Tytgat, J., and Hess, P. (1992). Subunit stoichiometry of a mammalian K^+ channel determined by construction of multimeric cDNAs. Neuron *9*, 861–871.

Long, S.B., Campbell, E.B., and Mackinnon, R. (2005a). Crystal structure of a mammalian voltage-dependent Shaker family K^+ channel. Science *309*, 897–903.

Long, S.B., Campbell, E.B., and Mackinnon, R. (2005b). Voltage sensor of Kv1.2: structural basis of electromechanical coupling. Science *309*, 903–908.

Lu, Z., Klem, A.M., and Ramu, Y. (2001). Ion conduction pore is conserved among potassium channels. Nature *413*, 809–813.

Lu, Z., Klem, A.M., and Ramu, Y. (2002). Coupling between voltage sensors and activation gate in voltage-gated K^+ channels. J. Gen. Physiol. *120*, 663–676.

Mannuzzu, L.M., and Isacoff, E.Y. (2000). Independence and cooperativity in rearrangements of a potassium channel voltage sensor revealed by single subunit fluorescence. J. Gen. Physiol. *115*, 257–268.

Monks, S.A., Needleman, D.J., and Miller, C. (1999). Helical structure and packing orientation of the S2 segment in the shaker K^+ channel. J. Gen. Physiol. *113*, 415–423.

Murata, Y., Iwasaki, H., Sasaki, M., Inaba, K., and Okamura, Y. (2005). Phosphoinositide phosphatase activity coupled to an intrinsic voltage sensor. Nature *435*, 1239–1243.

Papazian, D.M., Shao, X.M., Seoh, S.A., Mock, A.F., Huang, Y., and Wainstock, D.H. (1995). Electrostatic interactions of S4 voltage sensor in Shaker K^+ channel. Neuron *14*, 1293–1301.

Pathak, M., Kurtz, L., Tombola, F., and Isacoff, E. (2005). The cooperative voltage sensor motion that gates a potassium channel. J. Gen. Physiol. *125*, 57–69.

Perozo, E., MacKinnon, R., Bezanilla, F., and Stefani, E. (1993). Gating currents from a nonconducting mutant reveal open-closed conformations in Shaker K^+ channels. Neuron *11*, 353–358.

Perozo, E., Santacruz-Toloza, L., Stefani, E., Bezanilla, F., and Papazian, D.M. (1994). S4 mutations alter gating currents of Shaker K^+ channels. Biophys. J. *66*, 345–354.

Piper, D.R., Sanguinetti, M.C., and Tristani-Firouzi, M. (2005). Voltage sensor movement in the hERG K+ channel. Novartis Found. Symp. *266*, 46–52.

Ramsey, I.S., Moran, M.M., Chong, J.A., and Clapham, D.E. (2006). A voltage-gated proton-selective channel lacking the pore domain. Nature *440*, 1213–1216.

Ramu, Y., Xu, Y., and Lu, Z. (2006). Enzymatic activation of voltage-gated potassium channels. Nature *442*, 696–699.

Santacruz-Toloza, L., Huang, Y., John, S.A., and Papazian, D.M. (1994). Glycosylation of shaker potassium channel protein in insect cell culture and in Xenopus oocytes. Biochemistry *33*, 5607–5613.

Sasaki, M., Takagi, M., and Okamura, Y. (2006). A voltage sensor-domain protein is a voltage-gated proton channel. Science *312*, 589–592.

Schoppa, N.E., and Sigworth, F.J. (1998a). Activation of shaker potassium channels. I. Characterization of voltage- dependent transitions. J. Gen. Physiol. *111*, 271–294.

Schoppa, N.E., and Sigworth, F.J. (1998b). Activation of Shaker potassium channels. II. Kinetics of the V2 mutant channel. J. Gen. Physiol. *111*, 295–311.

Schoppa, N.E., and Sigworth, F.J. (1998c). Activation of Shaker potassium channels. III. An activation gating model for wild-type and V2 mutant channels. J. Gen. Physiol. *111*, 313–342.

Schulteis, C.T., John, S.A., Huang, Y., Tang, C.Y., and Papazian, D.M. (1995). Conserved cysteine residues in the shaker K^+ channel are not linked by a disulfide bond. Biochemistry *34*, 1725–1733.

Seoh, S.A., Sigg, D., Papazian, D.M., and Bezanilla, F. (1996). Voltage-sensing residues in the S2 and S4 segments of the Shaker K^+ channel. Neuron *16*, 1159–1167.

Smith-Maxwell, C.J., Ledwell, J.L., and Aldrich, R.W. (1998a). Role of the S4 in cooperativity of voltage-dependent potassium channel activation. J. Gen. Physiol. *111*, 399–420.

Smith-Maxwell, C.J., Ledwell, J.L., and Aldrich, R.W. (1998b). Uncharged S4 residues and cooperativity in voltage-dependent potassium channel activation. J. Gen. Physiol. *111*, 421–439.

Starkus, J.G., Kuschel, L., Rayner, M.D., and Heinemann, S.H. (1998). Macroscopic Na^+ currents in the "Nonconducting" Shaker potassium channel mutant W434F. J. Gen. Physiol. *112*, 85–93.

Stefani, E., Toro, L., Perozo, E., and Bezanilla, F. (1994). Gating of Shaker K^+ channels: I. Ionic and gating currents. Biophys. J. *66*, 996–1010.

Sukhareva, M., Hackos, D.H., and Swartz, K.J. (2003). Constitutive activation of the shaker Kv channel. J. Gen. Physiol. *122*, 541–556.

Yang, Y., Yan, Y., and Sigworth, F.J. (1997). How does the W434F mutation block current in Shaker potassium channels? J. Gen. Physiol. *109*, 779–789.

Yellen, G. (2002). The voltage-gated potassium channels and their relatives. Nature *419*, 35–42.

Yifrach, O., and MacKinnon, R. (2002). Energetics of pore opening in a voltage-gated K^+ channel. Cell *111*, 231–239.

Zagotta, W.N., Hoshi, T., and Aldrich, R.W. (1990). Restoration of inactivation in mutants of Shaker potassium channels by a peptide derived from ShB. Science *250*, 568–571.

Zagotta, W.N., Hoshi, T., and Aldrich, R.W. (1994a). Shaker potassium channel gating. III: Evaluation of kinetic models for activation. J. Gen. Physiol. *103*, 321–362.

Zagotta, W.N., Hoshi, T., Dittman, J., and Aldrich, R.W. (1994b). Shaker potassium channel gating. II: Transitions in the activation pathway. J. Gen. Physiol. *103*, 279–319.